



HHS Public Access

Author manuscript

Bioorg Med Chem Lett. Author manuscript; available in PMC 2019 March 01.

Published in final edited form as:

Bioorg Med Chem Lett. 2018 March 01; 28(5): 858–862. doi:10.1016/j.bmcl.2018.02.011.

Design, synthesis, and discovery of 5-((1,3-diphenyl-1*H*-pyrazol-4-yl)methylene)pyrimidine-2,4,6(1*H*,3*H*,5*H*)-triones and related derivatives as novel inhibitors of mPGES-1

Kai Ding^{a,b,c,†}, Ziyuan Zhou^{a,b,†}, Shuo Zhou^{a,b,†}, Yaxia Yuan^{a,b,d}, Kyungbo Kim^{a,b}, Ting Zhang^{a,b}, Xirong Zheng^{a,b}, Fang Zheng^{a,b}, and Chang-Guo Zhan^{a,b,d,*}

^aMolecular Modeling and Biopharmaceutical Center, College of Pharmacy, University of Kentucky, 789 South Limestone Street, Lexington, KY 40536

^bDepartment of Pharmaceutical Sciences, College of Pharmacy, University of Kentucky, 789 South Lime-stone Street, Lexington, KY 40536

^cDepartment of Chemistry, University of Kentucky, 505 Rose Street, Lexington, KY 40506

^dCenter for Pharmaceutical Research and Innovation, College of Pharmacy, University of Kentucky, 789 South Limestone Street, Lexington, KY 40536

Abstract

Human mPGES-1 has emerged as a promising target in exploring a next generation of anti-inflammatory drugs, as selective mPGES-1 inhibitors are expected to discriminatively suppress the production of induced PGE₂ without blocking the normal biosynthesis of other prostanoids including homeostatic PGE₂. Therefore, this therapeutic approach is believed to reduce the adverse effects associated with the application of traditional non-steroidal anti-inflammatory drugs (tNSAIDs) and selective COX-2 inhibitors (coxibs). Identified from structure-based virtue screening, the compound with (*Z*)-5-benzylidene-2-iminothiazolidin-4-one scaffold was used as lead in rational design of novel inhibitors. Besides, we further designed, synthesized, and evaluated 5-((1,3-diphenyl-1*H*-pyrazol-4-yl)methylene)pyrimidine-2,4,6(1*H*,3*H*,5*H*)-triones and structurally related derivatives for their *in vitro* inhibitory activities. According to *in vitro* activity assays, a number of these compounds were capable of inhibiting human mPGES-1, with the desirable selectivity for mPGES-1 over COX isozymes.

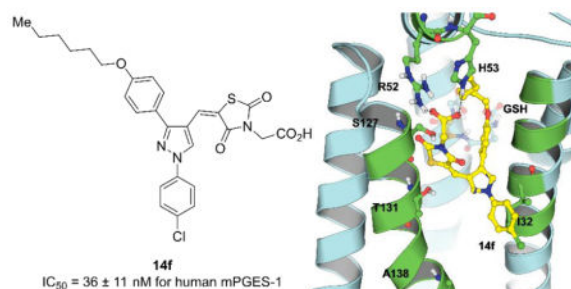
Graphical Abstract

Correspondence: Chang-Guo Zhan, Ph.D., Director, Molecular Modeling and Biopharmaceutical Center (MMBC), Director, Chemoinformatics and Drug Design Core of CPRI, University Research Professor, Endowed College of Pharmacy Professor in Pharmaceutical Sciences, Professor, Department of Pharmaceutical Sciences, College of Pharmacy, University of Kentucky, 789 South Limestone Street, Lexington, KY 40536, Phone: 859-323-3943, FAX: 859-257-7585, zhan@uky.edu.

[†]These authors contributed equally to this work.

Publisher's Disclaimer: This is a PDF file of an unedited manuscript that has been accepted for publication. As a service to our customers we are providing this early version of the manuscript. The manuscript will undergo copyediting, typesetting, and review of the resulting proof before it is published in its final citable form. Please note that during the production process errors may be discovered which could affect the content, and all legal disclaimers that apply to the journal pertain.

Rational molecular design, followed by synthesis and *in vitro* activity assays for evaluating both the potency and selectivity, has led to the discovery of a set of novel, potent and selective mPGES-1 inhibitors.



Keywords

Anti-inflammatory drugs; pyrazole; barbituric acid; mPGES-1 inhibitor

In the eicosanoid pathway, arachidonic acid (AA) is converted to prostaglandin H₂ (PGH₂) by the action of cyclooxygenases (COX-1 and COX-2). PGH₂ serves as a common precursor for various biologically active prostanoids, such as thromboxane A₂ (TXA₂), PGD₂, PGI₂, PGF_{2 α} , and PGE₂, depending on different distal synthases.^{1, 2} Among these prostanoids, PGE₂ is well recognized as an important inflammatory mediator. PGE₂ is isomerized from PGH₂ catalyzed by three distinct synthases, including microsomal prostaglandin E₂ synthase-1 (mPGES-1), mPGES-2, and cytosolic prostaglandin E₂ synthase.³ Unlike the other two constitutively expressed enzymes, the expression of mPGES-1, similar to that of COX-2, is highly inducible in response to pro-inflammatory stimuli.⁴

As two generations of anti-inflammatory drugs, traditional non-steroidal anti-inflammatory drugs (tNSAIDs) and coxibs represent the mainstream for the treatment of inflammation-related symptoms by either non-selectively inhibiting COX isozymes,⁵ or selectively inhibiting COX-2,⁶ respectively. However, both categories shut down the biosynthesis of all downstream prostanoids and, so, their application is associated with considerable adverse effects. The tNSAIDs trigger gastrointestinal (GI) ulceration because of the interference with COX-1-derived protective function in GI tract;⁷ coxibs, as specific COX-2 inhibitors, on the other hand, break the internal balance of vasodilative PGI₂ and vasoconstrictive TXA₂ and thus result in cardiovascular risk.⁸ Since PGE₂ is the major inducible PG in inflammation, inhibiting mPGES-1 is believed as a promising therapeutic approach in the development of the next generation of anti-inflammatory drugs.⁹

In the previous study, we reported the discovery of (*Z*)-5-benzylidene-2-iminothiazolidin-4-one derivative **1** (Figure 1A) as a human mPGES-1 inhibitor with moderate potency ($IC_{50} = 3.5$ μ M) through structure-based virtual screening.^{10, 11} Based on the simulated binding mode of **1** with crystal structure (PDB ID: 4BPM,¹² Figure 1B) of human mPGES-1, we redesigned the core scaffold and synthesized benzylidenebarbituric acid derivatives (**2**, with $IC_{50} = 622$ nM, as an example, Figure 1A) as mPGES-1 inhibitors. The barbituric acid was introduced in order to maintain and possibly enhance the polar interaction with the enzyme

at the active site. Flexible alkoxy side chain was attached to the central benzene ring so as to fit the size of the hydrophobic pocket surrounded by I32, G35, L39, Y130, T131, L135, and A138. As predicted by molecular docking, the barbituric ring interacts with S127 by forming a hydrogen bond (HB) between the barbituric carbonyl group and hydroxyl group of serine, while the central benzene ring with alkoxy substitution occupies the hydrophobic groove where the long hydrocarbon “tail” of PGH₂ locates (Figure 1C).

While developing the benzylidenebarbituric acid derivatives, we carefully analyzed the binding mode of these compounds with mPGES-1, and noticed that there is still substantial unoccupied area in the active site, especially the small hydrophobic pocket around the central benzene ring of **2** and above the cofactor glutathione (GSH) of the enzyme. We then decided to introduce pyrazole into the core scaffold not only because of its existence in many bioactive molecules, but also its versatility for multi-functionalization. We kept the barbituric acid “head” because of the importance of the hydrogen bond between carbonyl and hydroxyl group of S127. Substituents on pyrazole-1 and 3 positions were expected to occupy the hydrophobic pockets wrapping the hydrocarbon “tail” of PGH₂ and above GSH. Thus, a series of 5-((1,3-diphenyl-1*H*-pyrazol-4-yl)methylene)pyrimidine-2,4,6 (1*H*,3*H*,5*H*)-trione derivatives and other structurally related compounds were designed and synthesized. The docking study of the simplest scaffold **3** (Figure 1A) with mPGES-1 revealed that **3** binds in a similar region in the active site as **2** in the binding complex (Figure 1D). The strategies of improving the inhibitory efficacy in light of the binding complex include the modification on barbituric acid moiety for maintaining and strengthening a hydrogen bond with S127, and the substitution on 1- and/or 3-phenyl in order to enhance the hydrophobic interaction with the nonpolar groove. As expected, a number of these compounds were active against human mPGES-1 and selective for mPGES-1 over COX isozymes.

The synthesis of this series of compounds followed a straightforward multi-step protocol, as shown in Scheme 1. 4-Alkoxyacetophenone (**4b~4g**), obtained from the reaction of 4-hydroxyacetophenone and alkyl bromide,¹³ or acetophenone (**4a**) was condensed with 4-chlorophenylhydrazine in reflux ethanol containing 5 % glacial acetic acid.^{14, 15} The ethylidene hydrazine (**5a~5g**) was formed as precipitate at room temperature and filtered off. The next step was Vilsmeier-Haack-Arnold ring closing formylation,¹³ by treating **5a~5g** with POCl₃/DMF. The produced 1*H*-pyrazole-4-carbaldehyde intermediate (**6a~6g**) was coupled with barbituric acid or 2-thiobarbituric acid in refluxing EtOH/H₂O (4:1, v/v) to afford the final product (**7a~7g** or **8a~8g**).¹⁶

The length and shape of the aliphatic side chain were investigated in the SAR study. We fixed the substituent at pyrazole-1-position as 4-chlorophenyl and varied the side chain on 3-phenyl. From the *in vitro* data shown in Table 1, it was observed as compared to that without a side chain (**7a** and **8a**), compounds with linear side chains (**7b~7f** and **8b~8f**) were generally more potent against human mPGES-1, whereas benzyl substitution (**7g** and **8g**), however, did not improve the inhibitory potency. Linear side chains with 4 or 6 carbons yielded compounds with highest potency, whereas longer side chains, such as octyl or decyl, did not show a more potent inhibition. Notably, compounds with 2-thiobarbituric acid “heads” were generally more potent as compared to those with barbituric acid ones. We also changed the substituent in pyrazole-1-position from 4-chlorophenyl to phenyl group. In this

case, **4c** was used as starting substituted acetophenone. Followed the similar protocol as outlined in Scheme 2, **11** and **12** were prepared. These compounds (**11** and **12**) were slightly less potent than those with 4-chlorophenyl substituent (**7c** and **8c**, respectively).

With these (2-thio)barbituric acid derivatives in hand, as depicted in Scheme 3, we broadened the structural diversity with pyrazole core by coupling 1*H*-pyrazole-4-carbaldehydes (**6b** and **6d**) with various activated methylene compounds such as malononitrile, 2-cyanoacetic acid and 2,4-thiazolidinedione. As shown in Table 2, compounds with malononitrile and 2-cyanoacetamide “heads” (**13b**, **13c** and **14b**, **14c**) were not very active against human mPGES-1, whereas those with 2-cyanoacetic acid (**13a** and **14a**) showed submicromolar potency. It was noted that compounds **13f** and **14f**, obtained from the coupling of **6b** and **6d** with 2,4-thiazolidinedione *N*-acetic acid, were capable of inhibiting human mPGES-1 with low nanomolar potency (IC₅₀ = 41 ± 5 nM and 36 ± 11 nM, respectively).

To further understand the SAR of these synthesized compounds, we selected compounds **7c**, **7e** and **14f** and used the AutoDock Vina program¹⁷ as the molecular docking tool to investigate their binding modes with human mPGES-1. **14f** was chosen for further docking study because it is the most active one with the scaffold (possessing a carboxylic acid polar “head”) for the mPGES-1 inhibitors in Table 2. **7c** and **7e** were chosen from compounds in Table 1 with another scaffold (barbituric acid derivatives). Of the barbituric acid derivatives in Table 1, we are mainly interested in the compounds with Y = O, because the compounds with Y = S are less soluble in water. Within all of the barbituric acid derivatives with Y = O in Table 1, **7c** is the most potent one for human mPGES-1. **7e** was also chosen for comparison with **7c** because they are different only in the length of the side chain (R²).

The predicted binding modes are shown in Figure 2. The substituted phenyl group on pyrazole-1-position occupies the hydrophobic groove where the long hydrocarbon side chain of PGH₂ locates. The other substituted phenyl group on pyrazole-3-position fits into the small hydrophobic pocket above GSH. Since this pocket is small, a bulky group on pyrazole-3-position is not favorable as reflected in the inhibitory data that **7e** (with longer octyl side chain) is an inferior inhibitor as compared with **7c** (with a shorter butyl side chain). The substituents on pyrazole-4-position attaches on the surface of the protein. When the barbituric acid is present, the carbonyl group on the barbituric ring forms a hydrogen bond with the hydroxyl group of S127. While replacing the barbituric acid with 2,4-thiazolidinedione *N*-acetic acid, however, the carboxyl group forms hydrogen bonds with the NH groups of R52 and H53. So, **14f** is a potent inhibitor against human mPGES-1.

For the *in vitro* evaluation of these compounds, we first conducted the single-concentration screening at 10 μM against human mPGES-1. Compounds that showed significant inhibition (> 70%) were tested further for their IC₅₀ values against human mPGES-1. The protocol for the protein preparation and *in vitro* activity assays were the same as described previously.^{10, 11, 18, 19} Further, the inhibitory activity against COX isozymes was also evaluated for some of the more promising compounds (with IC₅₀ < 100 nM against human mPGES-1). As shown in Table 3, at a concentration as high as 100 μM, compounds **8b-8f**, **12**, **13f**, **14a** and

14f inhibited COX-1/2 for less than 20 %. So, these compounds are highly selective for the mPGES-1 over COX-1/2.

In summary, in light of the binding complex of both the lead and the benzylidenebarbituric acid scaffold with human mPGES-1, we designed and synthesized a novel series of 5-((1,3-diphenyl-1*H*-pyrazol-4-yl)methylene)-pyrimidine-2,4,6 (1*H*,3*H*,5*H*)-triones and other structurally related derivatives.²⁰ These compounds were evaluated *in vitro* for their inhibitory potency against human mPGES-1 and selectivity over COX-1/2, leading to discovery of various potent and selective inhibitors of human mPGES-1. The most potent one is **14f** (IC₅₀ = ~36 nM against human mPGES-1) without significant inhibition against COX-1/2.

Acknowledgments

This work was supported in part by the funding of the Molecular Modeling and Biopharmaceutical Center at the University of Kentucky College of Pharmacy, the National Science Foundation (NSF grant CHE-1111761), and the National Institutes of Health *via* the National Center for Advancing Translational Sciences (UL1TR001998) grant. The authors also acknowledge the Computer Center at University of Kentucky for supercomputing time on a Dell Supercomputer Cluster consisting of 388 nodes or 4,816 processors.

REFERENCES AND NOTES

1. Norberg JK, Sells E, Chang HH, Alla SR, Zhang S, Meuillet EJ. *Pharm Pat Anal.* 2013; 2:265. [PubMed: 24237030]
2. Garavito RM, DeWitt DL. *Biochim Biophys Acta.* 1999; 1441:278. [PubMed: 10570255]
3. Murakami M, Nakatani Y, Tanioka T, Kudo I. *Prostaglandins Other Lipid Mediat.* 2002; 68–69:383.
4. Funk CD. *Science.* 2001; 294:1871. [PubMed: 11729303]
5. Samuelsson B, Morgenstern R, Jakobsson PJ. *Pharmacol Rev.* 2007; 59:207. [PubMed: 17878511]
6. Hawkey CJ. *Best Pract Res Clin Gastroenterol.* 2001; 15:801. [PubMed: 11566042]
7. FitzGerald GA, Patrono C. *N Engl J Med.* 2001; 345:433. [PubMed: 11496855]
8. Buttgerit F, Burmester GR, Simon LS. *Am J Med.* 2001; 110(Suppl 3A):13S. [PubMed: 11173045]
9. Cheng Y, Wang M, Yu Y, Lawson J, Funk CD, Fitzgerald GA. *J Clin Invest.* 2006; 116:1391. [PubMed: 16614756]
10. Hamza A, Zhao X, Tong M, Tai HH, Zhan CG. *Bioorg Med Chem.* 2011; 19:6077. [PubMed: 21920764]
11. Zhou Z, Yuan Y, Zhou S, Ding K, Zheng F, Zhan CG. *Bioorg Med Chem Lett.* 2017; 27:3739. [PubMed: 28689972]
12. Li D, Howe N, Dukkipati A, Shah ST, Bax BD, Edge C, Bridges A, Hardwicke P, Singh OM, Giblin G, Pautsch A, Pfau R, Schnapp G, Wang M, Olieric V, Caffrey M. *Cryst Growth Des.* 2014; 14:2034.
13. Yamasaki K, Hishiki R, Kato E, Kawabata J. *ACS Med Chem Lett.* 2011; 2:17. [PubMed: 24900249]
14. Ragab FA, Abdel Gawad NM, Georgey HH, Said MF. *Eur J Med Chem.* 2013; 63:645. [PubMed: 23567953]
15. Harikrishna N, Isloor AM, Ananda K, Obaid A, Fun HK. *RSC Advances.* 2015; 5:43648.
16. Baron R, Huang CH, Bassani DM, Onopriyenko A, Zayats M, Willner I. *Angew Chem Int Ed Engl.* 2005; 44:4010. [PubMed: 15912548]
17. Trott O, Olson AJ. *J Comput Chem.* 2010; 31:455. [PubMed: 19499576]
18. Hamza A, Tong M, AbdulHameed MD, Liu J, Goren AC, Tai HH, Zhan CG. *J Phys Chem B.* 2010; 114:5605. [PubMed: 20369883]

19. Huang XQ, Yan WL, Gao DQ, Tong M, Tai HH, Zhan CG. *Bioorg Med Chem.* 2006; 14:3553. [PubMed: 16439136]
20. Analytical data and yields for the most potent compounds: (13f) ^1H NMR (400 MHz, DMSO) δ 13.47 (s, 1H), 8.76 (s, 1H), 8.05 (d, $J=8.7$ Hz, 2H), 7.68 (s, 1H), 7.57 (dd, $J=26.7, 8.6$ Hz, 4H), 7.09 (d, $J=8.6$ Hz, 2H), 4.35 (s, 2H), 4.10 (q, $J=6.9$ Hz, 2H), 1.36 (t, $J=6.9$ Hz, 3H). ^{13}C NMR (101 MHz, DMSO) δ 168.00, 166.61, 164.74, 159.29, 153.83, 137.53, 131.57, 130.03, 129.48, 128.35, 124.12, 123.13, 120.93, 119.57, 115.31, 114.84, 63.24, 42.37, 14.63. HRMS (ESI $^+$) m/z calcd for $\text{C}_{23}\text{H}_{19}\text{ClN}_3\text{O}_5\text{S}$ (MH) $^+$: 484.0728, found: 484.0728. Yield: 74 %. (14f) ^1H NMR (400 MHz, DMSO) δ 8.78 (s, 1H), 8.06 (d, $J=8.8$ Hz, 2H), 7.69 (s, 1H), 7.63 (s, 1H), 7.61 – 7.47 (m, 3H), 7.09 (d, $J=8.7$ Hz, 2H), 4.36 (s, 2H), 4.03 (t, $J=6.5$ Hz, 2H), 1.82 – 1.64 (m, 2H), 1.48 – 1.28 (m, 6H), 0.88 (t, $J=6.8$ Hz, 3H). ^{13}C NMR (101 MHz, DMSO) δ 168.01, 166.62, 164.75, 159.47, 153.86, 137.55, 131.59, 130.04, 129.50, 128.40, 124.15, 123.13, 120.97, 119.59, 115.32, 114.90, 67.64, 42.34, 31.03, 28.63, 25.21, 22.11, 13.95. HRMS (ESI $^+$) m/z calcd for $\text{C}_{27}\text{H}_{27}\text{ClN}_3\text{O}_5\text{S}$ (MH) $^+$: 540.1354, found: 540.1352. Yield: 71 %.

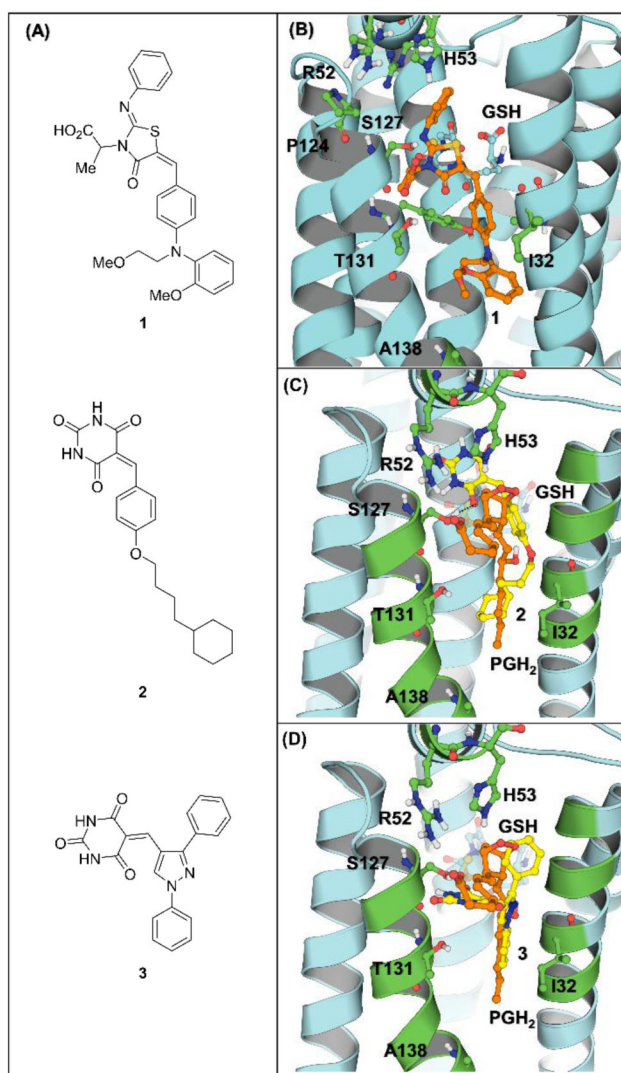


Figure 1. Molecular structures of the lead **1**, benzylidenebarbituric acid derivative **2** and the designed scaffold **3** and their binding with human mPGES-1. (A) Ligand structures; (B) binding with the lead **1**; (C) binding with **2**; (D) binding with **3**.

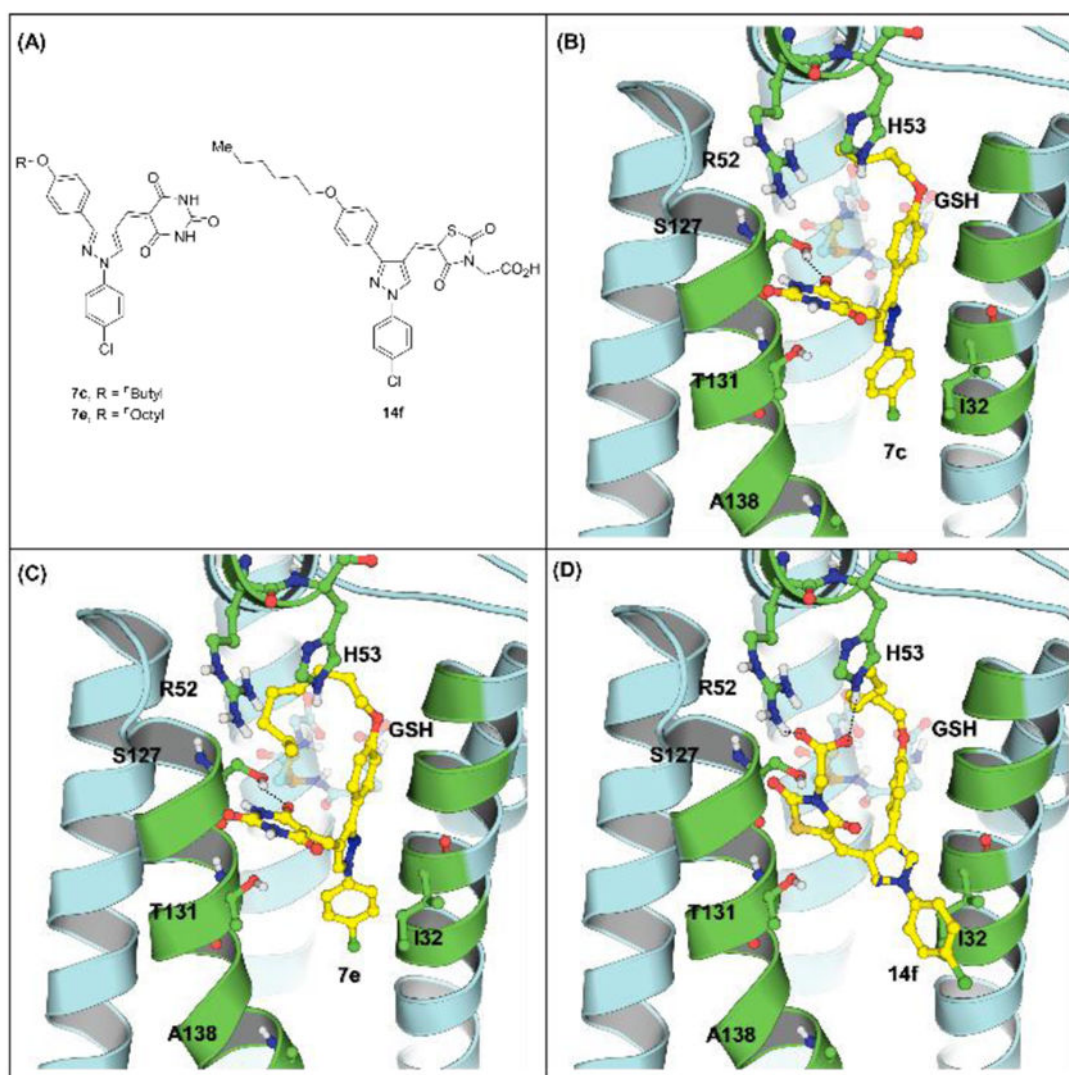
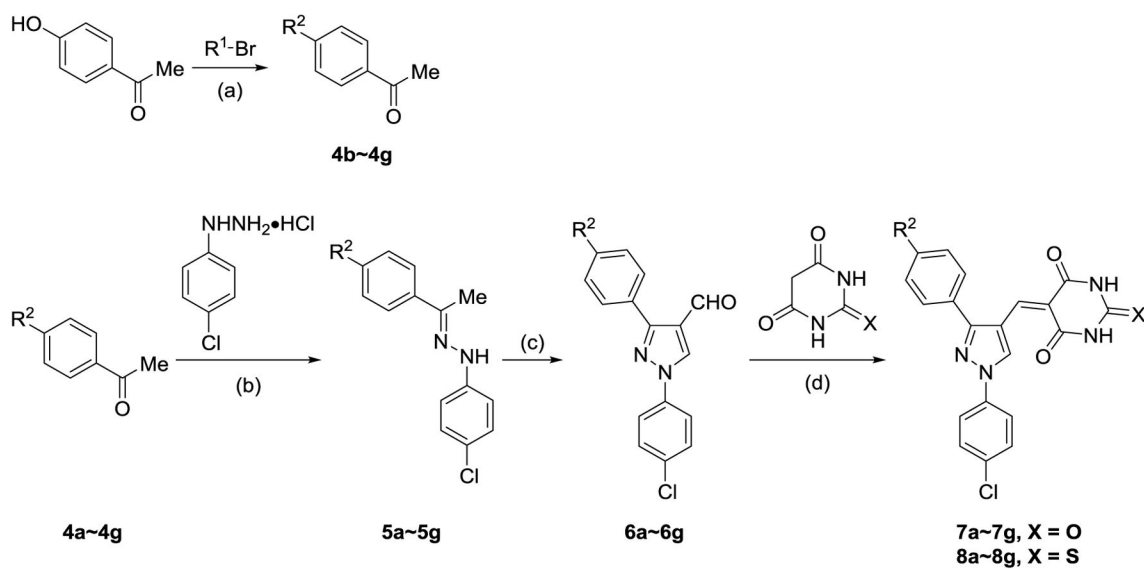
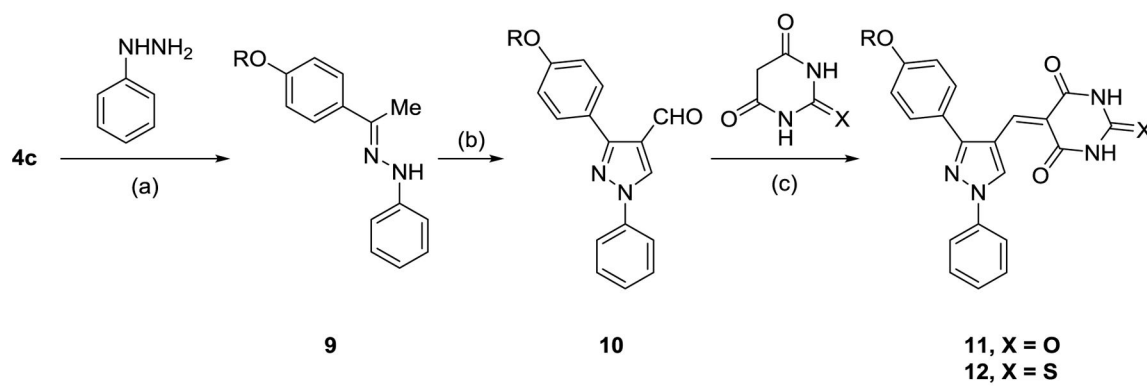


Figure 2. Molecular structures of **7c**, **7e** and **14f** and their binding with human mPGES-1. (A) Compound structures; (B) binding with the lead **7c**; (C) binding with **7e**; (D) binding with **14f**.

**Scheme 1.**

Reagents and conditions: (a) K_2CO_3 (2.00 equiv.), DMF, 80 °C; (b) 5 % glacial AcOH in EtOH, reflux; (c) $POCl_3$ (4.00 equiv.), DMF, 0 °C~60 °C; (d) EtOH/ H_2O (4:1, v/v), reflux.

**Scheme 2.**

Reagents and conditions: (a) 5 % glacial AcOH in EtOH, reflux; (b) POCl₃ (4.00 equiv.), DMF, 0 °C~60 °C; (c) EtOH/H₂O (4:1, v/v), reflux.

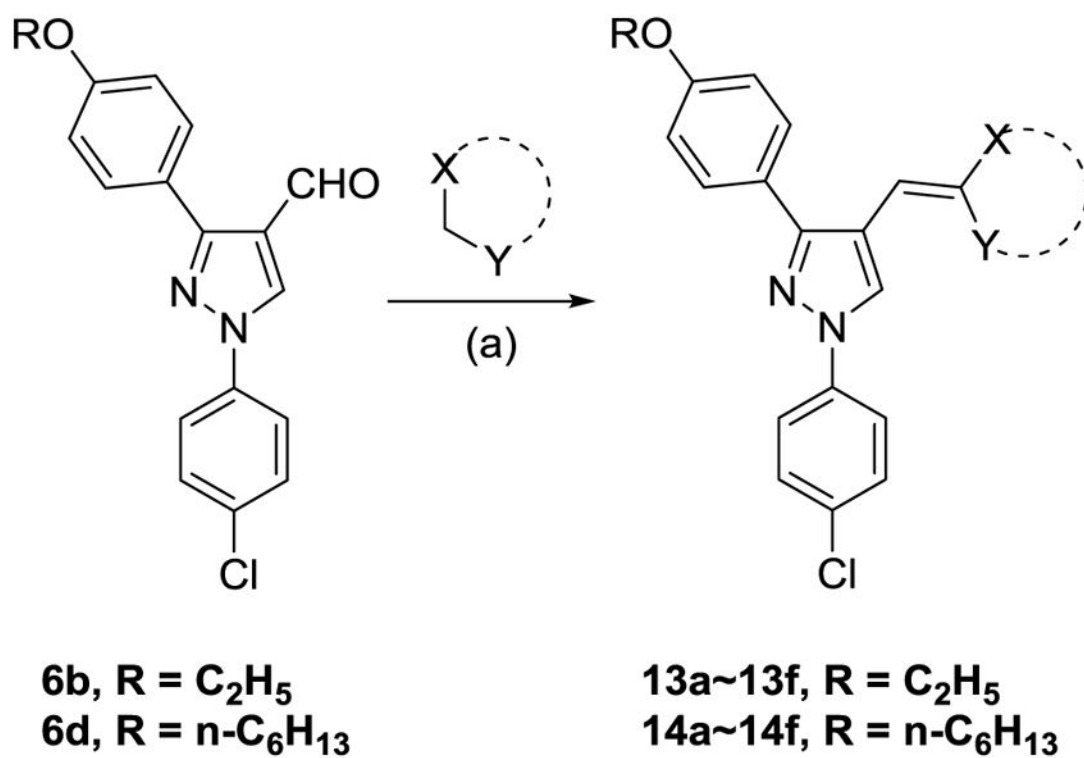
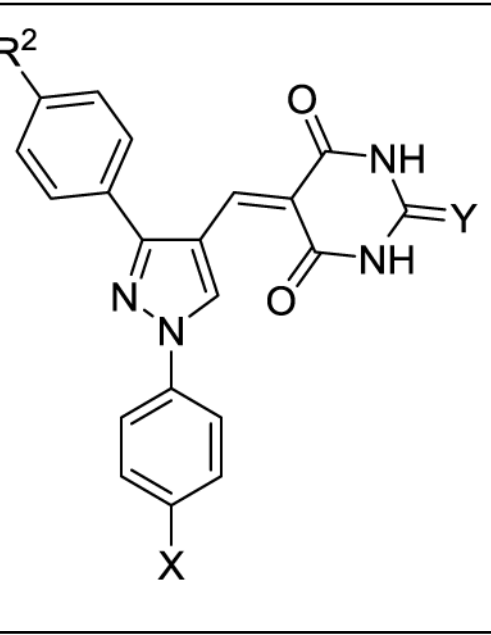
**Scheme 3.**Reagents and conditions: (a) NH₄OAc (2.00 equiv.), glacial AcOH, 108 °C.

Table 1

Structural-activity relationship (SAR) on the substitution of central pyrazole ring



The chemical structure shows a central pyrazole ring. At the 3-position of the pyrazole, there is a phenyl ring with a substituent R². At the 5-position, there is a phenyl ring with a substituent X. At the 4-position, there is a side chain consisting of a trans-alkene connected to a five-membered heterocyclic ring (pyrazolidinone). The heterocyclic ring has a carbonyl group (=O) at the 2-position, an NH group at the 3-position, and a substituent Y at the 4-position.

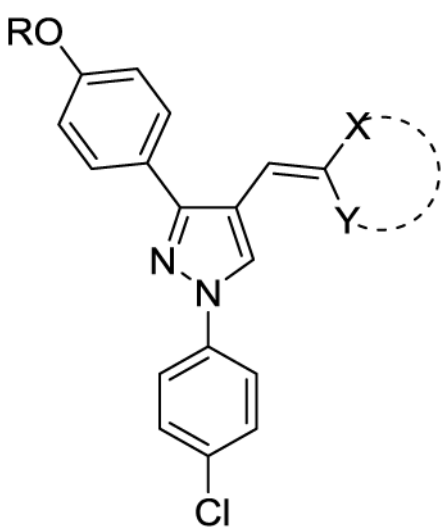

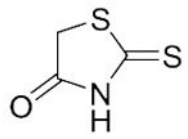
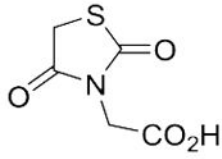
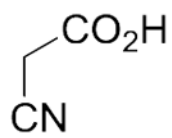
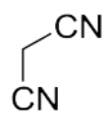
Comp.	R ²	X	Y	IC ₅₀ (nM) ^a for mPGES-1
7a	H	Cl	O	337±85
7b	C ₂ H ₅ O	Cl	O	265±96
7c	ⁿ C ₄ H ₉ O	Cl	O	169±41
7d	ⁿ C ₆ H ₁₃ O	Cl	O	285±65
7e	ⁿ C ₈ H ₁₇ O	Cl	O	361±51
7f	ⁿ C ₁₀ H ₂₁ O	Cl	O	294±83
7g	BnO	Cl	O	598±142
8a	H	Cl	S	561±192
8b	C ₂ H ₅ O	Cl	S	95±16
8c	ⁿ C ₄ H ₉ O	Cl	S	56±10
8d	ⁿ C ₆ H ₁₃ O	Cl	S	52±15
8e	ⁿ C ₈ H ₁₇ O	Cl	S	92±19
8f	ⁿ C ₁₀ H ₂₁ O	Cl	S	93±14
8g	BnO	Cl	S	797±160
11	ⁿ C ₄ H ₉ O	H	O	212±34
12	ⁿ C ₄ H ₉ O	H	S	92±20

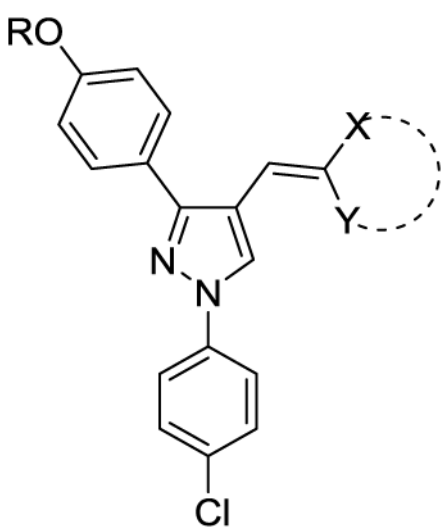

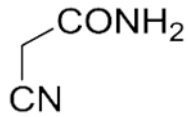
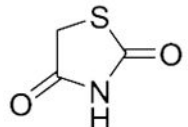
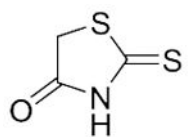
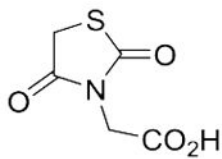
^aData are expressed as means ± SD (standard deviation) of single determinations obtained in triplicate.

Table 2

The SAR on the polar head

Comp.	R		IC ₅₀ (nM) ^a for mPGES-1
13a	C ₂ H ₅		283±83
13b	C ₂ H ₅		n.d. ^b (51%±10%) ^c
13c	C ₂ H ₅		n.d. (32%±21%)
13d	C ₂ H ₅		1,590±560

			
Comp.	R		IC ₅₀ (nM) ^a for mPGES-1
13e	C ₂ H ₅		1,040±290
13f	C ₂ H ₅		41±5
14a	ⁿ C ₆ H ₁₃		83±34
14b	ⁿ C ₆ H ₁₃		n.d. (64%±1.4%)

			
Comp.	R		IC ₅₀ (nM) ^a for mPGES-1
14c	ⁿ C ₆ H ₁₃		n.d. (14%±14%)
14d	ⁿ C ₆ H ₁₃		1,390±300
14e	ⁿ C ₆ H ₁₃		1,730±670
14f	ⁿ C ₆ H ₁₃		36±11

^aData are expressed as means ± SD (standard deviation) of single determinations obtained in triplicate.

^bn.d. = not determined.

^cThe value in the parenthesis refers to the % inhibition of the compound at a concentration of 10 μ M against the mPGES-1 (IC₅₀ values were determined only for the compounds that showed \geq 70% inhibition).

Author Manuscript

Author Manuscript

Author Manuscript

Author Manuscript

Table 3

Inhibition against COX-1/2

Compound	% Inhibition of COX-1/2 at 100 μ M ^a
8b	1.0 \pm 4.5
8c	4.4 \pm 8.6
8d	0.7 \pm 5.4
8e	0 \pm 0.2
8f	11 \pm 16
12	16 \pm 4.1
13f	6.8 \pm 6.4
14a	19 \pm 0.1
14f	1.2 \pm 29

^aThe % inhibition of the compound at a concentration of 100 μ M against the COX-1/2 (mixed COX-1 and COX-2). The enzyme mixture contained equal amounts of COX-1 and COX-2 in terms of their enzyme activities. In this way, when a compound can significantly inhibit either COX-1 or COX-2, it will show the significant inhibitory effects against the mixed COX-1 and COX-2.